Heartbeat-Induced Axial Motion Artifacts in Optical Coherence Tomography Measurements of the Retina

Roy de Kinkelder,[1,2] *Jeroen Kalkman,*[1] *Dirk J. Faber,*[1,3] *Olaf Schraa,*[4] *Pauline H. B. Kok,*[3] *Frank D. Verbraak,*[1,3] *and Ton G. van Leeuwen*[1,5]

Purpose. To investigate the cause of axial eye motion artifacts that occur in optical coherence tomography (OCT) imaging of the retina. Understanding the cause of these motions can lead to improved OCT image quality and therefore better diagnoses.

Methods. Twenty-seven measurements were performed on 5 subjects. Spectral domain OCT images at the macula were collected over periods up to 30 seconds. The axial shift of every average A-scan was calculated with respect to the previous average A-scan by calculating the cross-correlation. The frequency spectrum of the calculated shifts versus time was determined. The heart rate was determined from blood pressure measurements at the finger using an optical blood pressure detector. The fundamental frequency and higher order harmonics of the axial OCT shift were compared with the frequency spectrum of blood pressure data. In addition, simultaneous registration of the movement of the cornea and the retina was performed with a dual reference arm OCT setup, and movements of the head were also analyzed.

Results. A correlation of 0.90 was found between the fundamental frequency in the axial OCT shift and the heart rate. Cornea and retina move simultaneously in the axial direction. The entire head moves with the same amplitude as the retina.

Conclusions. Axial motion artifacts during OCT volume scanning of the retina are caused by movements of the whole head induced by the heartbeat. (*Invest Ophthalmol Vis Sci.* 2011;52: 3908–3913) DOI:10.1167/iovs.10-6738

Motion artifacts in medical imaging have been a topic of great interest for many years. Motion artifacts during image acquisition of a patient can be caused by muscular, peristaltic, cardiovascular, and/or respiratory activity.[1] Degradation of image quality resulting from motion can lead to ambiguous clinical interpretation and even erroneous diagnoses.[2] Investigating the causes of these involuntary motions can lead to a better understanding of the underlying physiology and improve clinical interpretation. Moreover, information of the origin of the motions can be used for image correction either during or after imaging.[3] Although motion artifacts are mostly considered disturbing, they can also contain valuable functional information on the patients' health state.

Optical coherence tomography (OCT) is a noninvasive, high-resolution optical imaging technique that is increasingly used in clinical practice.[4] OCT generates cross-sectional (B-scan) and 3-dimensional (3D) images by measuring echo time delay of backscattered light using interferometery.[5] Its main application is in ophthalmology; however, OCT is also applied in fields such as cardiovascular imaging,[6] dermatology,[7] gastroenterology,[8] and urology.[9] In ophthalmology, OCT is mainly used for imaging the central retina, where the retina–vitreous interface, sub- and intramacular edema,[10] and the retinal thickness[11] can be monitored. Around the optic nerve, the thickness of the nerve fiber layer (NFL) is especially important for diagnosis and follow-up of glaucoma patients.[11] In addition to morphologic imaging, OCT also can provide information about (retinal) blood flow using the Doppler shift of the backscattered light. Moving red blood cells cause a Doppler frequency shift of the backscattered light from which the speed of the moving particle can be derived.[12]

For OCT imaging of the retina, motion artifacts can be easily removed by using image alignment in image postprocessing. For Doppler OCT, bulk motions by the sample need to be corrected to accurately determine the absolute blood flow velocity.[13] With the higher imaging speeds (of >100,000 A-lines per second)[14] that are reached in Fourier domain OCT,[15–17] some of these motion artifacts have been ameliorated. Even in these systems, however, movements by a patient can still cause significant image quality degradation[18,19] and can be clearly visible in 3D OCT volume scans of the entire retina.

When OCT is used to visualize the retina, movements toward and away from the laser beam (axial movements) are often visible during acquisition of subsequent cross-sectional images, B-scans, in the so-called slow scanning direction in a 3D or volume scan. Figure 1 shows a typical 3D scan of the macula (3D OCT-1000 Mark I; Topcon, Capelle aan den IJssel, The Netherlands; 3.6 seconds acquisition time) made in our clinic. The slow scanning direction is indicated with an X. The axial motion of the retina is clearly visible as an oscillation of the retina–vitreous interface.

In this study, we first investigate the relation between axial motions visible in OCT scans of the retina and the heart rate of the subject by simultaneous OCT measurements and noninvasive optical blood pressure measurements on the finger from which the heart rate is derived. Second, simultaneous registration of the axial movement of the cornea and the retina is performed using a dual reference arm OCT setup. Third, we

From the Departments of [1]Biomedical Engineering & Physics and [3]Ophthalmology, Academic Medical Center, University of Amsterdam, Amsterdam, The Netherlands; [2]Topcon Europe Medical BV, Capelle aan den IJssel, The Netherlands; [4]BMEYE, Amsterdam, The Netherlands; [5]MIRA Institute for Biomedical Technology and Technical Medicine and Faculty of Science and Technology, Biomedical Photonic Imaging Group, University of Twente, Enschede, The Netherlands.

Supported by the IOP Photonics Devices Program managed by the technology foundations STW and SenterNovem (IPD067774). DJF is funded by a personal grant in the Vernieuwingsimpuls program (AGT07544) by the Netherlands Organisation of Scientific Research (NWO) and the Technology Foundation (STW). None of the authors have any financial or commercial interest in the tested devices.

Submitted for publication October 18, 2010; revised January 4, 2011; accepted March 16, 2011.

Disclosure: **R. de Kinkelder**, Topcon Europe Medical BV (E); **J. Kalkman**, None; **D.J. Faber**, None; **O. Schraa**, BMEYE BV (E); **P.H.B. Kok**, None; **F.D. Verbraak**, None; **T.G. van Leeuwen**, None

Corresponding author: Roy de Kinkelder, Academic Medical Center, University of Amsterdam, P.O. Box 22700, NL-1100 DE Amsterdam, The Netherlands; r.dekinkelder@amc.nl.

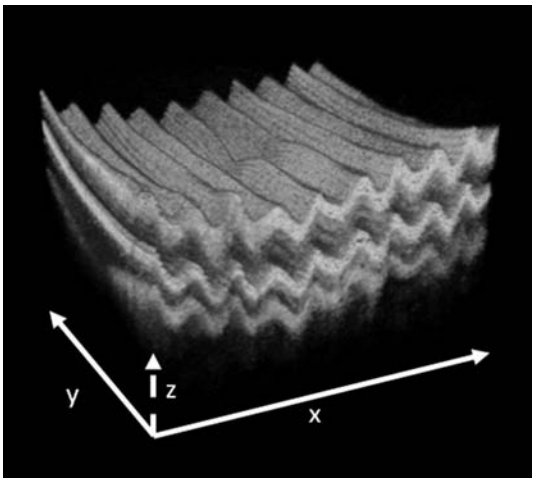

FIGURE 1. A 3D OCT image of the foveal region of the retina. The motion artifact in the axial direction (*z*-axis, *dashed arrow*) is clearly visible during scanning in the slow scanning direction (indicated with X). The OCT beam is incoming in *z* direction. Image size is: $x = 6$ mm (containing 128 b-scans), $y = 6$ mm (containing 512 depth scans), and $z = 2.6$ mm. Scan speed in this image was 18,000 Hz and was measured with Topcon 3D OCT-1000 Mark I.

investigate axial head movements with OCT scanning of the teeth. In addition, the axial position of the retina is recorded when a subject is lying down to decrease the influence of head movements.

MATERIALS AND METHODS

OCT Imaging Setup

We used a spectral domain OCT (SD-OCT; OCP840SR, Thorlabs GmbH, Munich, Germany) setup to image the human retina. The sample arm of the SD-OCT setup was adjusted to an ophthalmic configuration (i.e., the entrance beam in the sample arm was first collimated). To create a telescopic entrance beam, 2 objective lenses (L1 and L2 in Fig. 2) were placed at a distance of 2 focal lengths from each other. With the scan mirror in the focal point of L1, the pivot point of the collimated beam was situated in the pupil plane, resulting in a large field of view of the retina (no mydriatic was needed to dilate the pupil). The SD-OCT set up contained a super luminescent diode with a center wavelength of 848 nm and an optical bandwidth of 30 nm. The optical bandwidth limited axial resolution in air was 10.5 μm, and the measured axial resolution in air was 11.5 μm. The scan rate of the line scan camera system was 5000 lines per second. The sensitivity, defined as the ratio between the signal amplitude and the SD of the noise, was 104.9 dB at 200 μm from the zero path length difference location measured on a mirror placed in a model eye[20] and using an optical density filter. The measured 3-dB sensitivity roll off was at 1.2 mm from the zero delay point. The maximal imaging depth was 3.5 mm. The output power measured at the position of the cornea was <700 μW. We positioned the OCT setup on an optical table, with the chin rest mounted at the end of the sample arm onto the same optical table. The scanner is not directly attached to the chin rest, and the setup is not able to move.

To investigate the simultaneous axial movement of the retina and the cornea, a dual reference arm was implemented in the OCT setup[21] (see Fig. 2). The light in the reference arm was split by a 50-50 beam splitter cube into a reference arm set to a distance for corneal imaging and a reference arm set to a distance for retinal imaging. The difference in optical path length between both reference arms was matched to the axial length of the examined eye. Light in the sample arm was partly focused by a cylindrical lens (CL in Fig. 2II; $f = 2.3$ mm) to create 2 focal points (astigmatic focusing). One plane of the sample arm light beam was focused by the cylindrical lens onto the cornea. The collimated light in the perpendicular plane was focused by the human eye onto the retina. Light of both focal points was combined with light of both reference arms and projected on the spectrometer resulting in a combined OCT image of the cornea and the retina. The scan mirror (MS1) was kept stationary to image at the same position.

For measurement on the teeth, the cylindrical lens in the sample arm that was used for the simultaneous registration of the cornea and the retina was replaced with a spherical lens (L3 in Fig. 2III; $f = 50$ mm). The scan mirror (MS1) was kept stationary to measure on the same position at the teeth.

Heartbeat Measurement

To determine the heart rate, the blood pressure was measured simultaneously and continuously during OCT imaging using a blood pressure monitor (Nexfin; BMEYE; Amsterdam, The Netherlands). This device used a volume clamp method with a pressurized cuff around the finger of the subject to obtain continuous noninvasive blood pressure. The blood pressure waveform (sample frequency, 200 Hz) and derived parameters (e.g., heart rate) were stored to file after the measurement. At both the start and at the end of the OCT scanning, an electric trigger signal was send to the monitor, and the trigger signal was stored in the blood pressure dataset. In postprocessing, the data of these triggers were used to synchronize the blood pressure measurement with the OCT measurement.

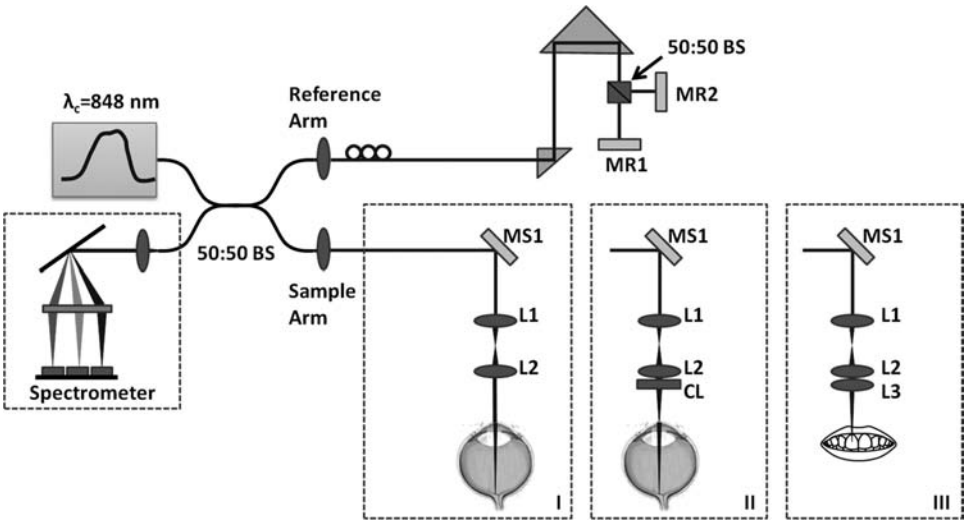

FIGURE 2. OCT setup with three (I, II, and III) sample arm configurations that are used for experiments on the retina, dual reference arm measurements, and measurements at the teeth, respectively. λ_c, central wavelength of light source; 50:50 BS, beamsplitter; MR, mirror reference arm; MS, scanning mirror sample arm; L, spherical lens; CL, cylindrical lens.

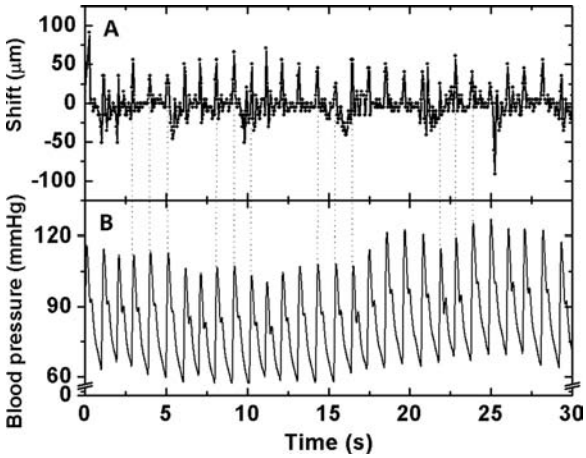

FIGURE 3. (**A**) The axial OCT shift of the retina, relative to $t = 0$, measured with OCT has an average peak-to-peak amplitude of 81 μm $\pm$ 3.5 μm. (**B**) Measured blood pressure at the index finger. The peak of the systole corresponds to the peak shift of the retina (indicated by *dashed vertical lines*).

Data Acquisition and Analysis

Consecutive cross-sectional OCT B-scans of the macula with a lateral scan length of 2.0 mm were collected in time. The time of acquisition of each B-scan was recorded. Each B-scan consisted of 40 axial depth scans (A-scans), which were summed to calculate an averaged A-scan. In this way, structural differences between consecutive images were minimized, and the signal-to-noise ratio and sample rate were increased. The axial OCT shifts were determined by a cross-correlation between the *i*-th and (*i*+*1*)-th averaged A-scan.[22] The position of the (*i*+*1*)-th averaged A-scan was aligned with the difference in position relative to the first averaged A-scan. The calculated total shifts, relative to the first averaged A-scan, were displayed versus time. A frequency spectrum of the averaged A-scan shift in time, with a minimal frequency resolution of 0.05 Hz, was determined to analyze its frequency content.

Measurements

To investigate the influence of the heartbeat on the axial motions, a total of 27 measurements was performed on 5 healthy subjects. The mean age of the subjects was 31 $\pm$ 8 years. All subjects were healthy without any known ocular pathology and with clear ocular media. The subjects were asked to fixate and relax while they placed their head on a chin rest. Furthermore, they were asked not to blink their eyes and to avoid large head movements. In the frequency spectrum of the axial OCT shift, peaks that were clearly visible above noise level were located manually and were analyzed. Peaks with frequencies lower than 0.5 Hz were excluded from analysis. The uncertainty in the central frequency of the peak is determined by the resolution of the frequency spectrum. From the blood pressure measurement, the corresponding part was selected using the start and stop triggers as a reference. A frequency spectrum was made of the blood pressure signal, and the fundamental frequency (i.e., the heart rate) was selected and used in further analysis.

Second, the movement of the retina and the cornea were measured simultaneously where the signal from the cornea was displayed in the upper part and the signal from the retina was displayed in the lower part of the B-scan image. Seventeen measurements were performed on 2 subjects. During these measurements, the scan mirror was not rotating. The average A-scan was segmented in a retinal image and a corneal image. The position analysis was performed on both images to determine the shift of the retina and the cornea.

Third, to register axial head motions, 10 measurements were performed on the teeth of 1 subject. The same cross-correlation method was used to calculate the axial OCT shift and to determine the frequency of the motion.

Finally, the effect of the heart rate on head motions was further investigated on 6 subjects who were asked to lie down, resting with the back side of the head on the floor during OCT imaging of the retina. In this way, head movements toward and away from the illuminating beam were restricted because gravity kept the head position constant. Five measurements per subject were performed in this position, and the same method was used in the analysis of the OCT images.

All research adhered to the tenets of the Declaration of Helsinki. We certify that all applicable institutional and governmental regulations concerning the ethical use of human volunteers were followed during this research.

RESULTS

Figure 3A shows a typical measurement of the axial shift of the retina versus time in 1 subject. A spiking axial motion with a period of approximately 1 second and average peak to peak amplitude of 81 μm $\pm$ 3.5 μm is observed. This spiking motion is observed in all subjects, albeit with some variability in amplitude and period. The slowly varying shift with a period of approximately 5 seconds in Figure 3A is attributed to breathing of the subject. The simultaneously measured blood pressure is displayed in Figure 3B. This graph shows a typical blood pressure waveform. The rise from diastolic pressure to the systolic blood pressure level (upstroke) is relatively sharp. During the decline to diastolic pressure, a local maximum can often be seen, which is caused by a reflection of the systolic pulse in the arterial tree (mainly in the abdomen of the subject). It can be easily observed that the peaks in the shift of the retina occur simultaneously with the peaks in the blood pressure. The frequency content of the OCT shift and blood pressure signals is shown in Figure 4A and 4B. In Figure 4A, the fundamental frequency of the OCT shift at 1 Hz and the higher harmonics of this fundamental frequency are clearly visible. The fundamental frequency of the motion artifact is 0.95 $\pm$ 0.02 Hz. The peak at 0.2 Hz in Figure 4A is the slowly varying shift that is caused by breathing. The fundamental frequency of the blood pressure is 0.95 $\pm$ 0.05 Hz, which is the heart rate. The fundamental and higher harmonic frequencies of the OCT shift and the fundamental frequency of the heart rate are used in subsequent analysis of the frequency spectra.

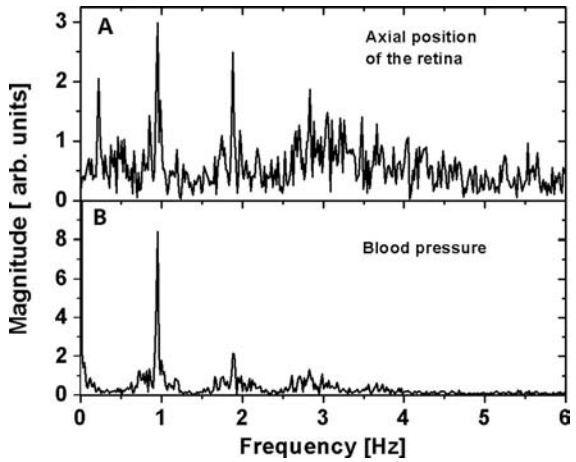

FIGURE 4. (**A**) Frequency spectrum of the axial shift of OCT images of the retina. (**B**) Frequency spectrum of the blood pressure pulse. Note that the higher order harmonics are visible in both the axial position of the retina and in the blood pressure.

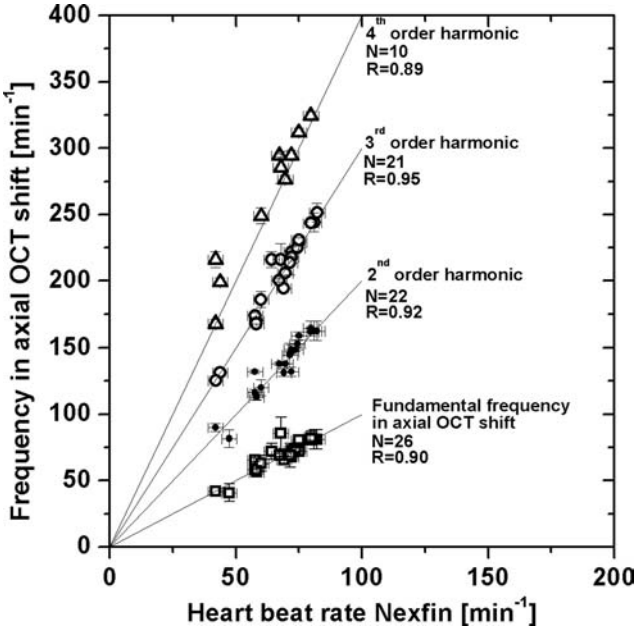

FIGURE 5. Frequency components of the axial OCT shift of the retina versus the fundamental frequency of the blood pressure, the heart rate. The fundamental frequency of the retinal (□) was identified in 26 measurements. There is a linear correlation between the fundamental frequency of the axial OCT shift and the heartbeat ($R = .90$). The second order harmonic of the axial position of the retina (●) versus the real heart rate was found in 22 measurements. The third order harmonic of the axial position of the retina (○) versus the real heart rate was determined in 21 measurements. The fourth order harmonic of the axial position of the retina (△) versus the real heart rate was determined in 10 measurements.

In Figure 5, all identified frequency components of the axial shift in the OCT image for 26 measurements (displayed in the figure with □) are plotted against the heart rate. The line trough the data are used as guide to the eye, with each line having a slope that is a multiple of the slope of the heart rate. The second order harmonic is visible in 21 measurements (displayed in the figure with ●), the third order harmonic is visible in 20 measurements (displayed in the figure with ○), and the fourth order harmonic of the axial shift of the retina (displayed in the figure with △) is visible in 10 measurements. We find a clear correlation between the heart rate and the fundamental frequency of the axial motion ($R = .90$) and also high correlations between the harmonics of the OCT shift and the heart rate ($R = .92$, $R = .95$, and $R = .89$ for the second, third, and fourth order harmonics, respectively).

Next, we investigate in a series of experiments what movement is causing the axial retinal motion.

First, we measure the axial shift of the cornea and retina simultaneously (see Fig. 6A). This measurement indicates that the cornea moves simultaneously with the retina because the phase of the signals is similar. However, the amplitude of the motion of the retina is larger than the amplitude of the motion of the cornea, especially in large amplitude excursions.

Second, the axial OCT shift measured on the teeth of 1 subject is displayed versus time in Figure 6B. The fundamental frequency in the OCT motion is at 0.8 Hz corresponding to the fundamental frequency of the heart rate of the subject. The amplitude has a similar magnitude as the amplitude measured on the retina: 89.0 ± 7.1 μm.

Third, subjects were lying down while OCT imaging is performed on the retina. The result of 1 measurement is displayed in Figure 6C. The motions have a mean peak-peak value of 21.3 ± 8.0 μm. It is clear that the amplitude of the motion in the lying down position is much smaller than the amplitude shown in Figure 6B. This was obtained for all subjects.

DISCUSSION

In this study, we have shown that the fundamental frequency in the axial motion of the retina and the heart rate are highly correlated. Figure 3 and the frequency analysis in Figure 4 show a typical measurement of the OCT shift and the blood pressure. The similar fundamental frequencies in the OCT shift and the blood pressure indicate that the heart rate causes the periodic axial shifts in the OCT images of the retina. The axial shift of the retina is clearly visible when the subject is situated quietly with their head positioned on the chin rest. Indicating that our home built OCT system is stable and sensitive enough to measure axial motions induced by the heart beat, validation measurements were performed on a static phantom eye model, with no axial motions visible.

In Figure 3 a low frequency movement is also visible, which we observed to be caused by whole body movement during breathing of the subject during acquisition of the OCT scan. Breathing causes a slow and small amplitude movement of the subject's head, which is resting on the chin rest. The frequency spectrum of Figure 4A shows that this movement has a frequency of 0.2 Hz, which is similar to typical breathing rates for humans in rest (around 12 times per minute). We therefore neglected the signals in the frequency analysis.

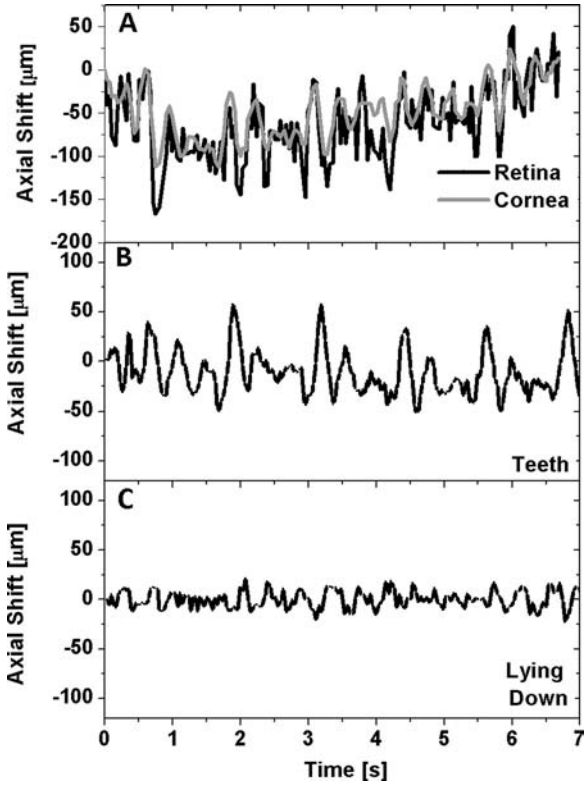

FIGURE 6. (**A**) Shift in axial direction of the retina (*black line*) and cornea (*gray line*) measured with a double reference arm OCT. (**B**) Typical measurement of the shift in the axial direction measured on the teeth of 1 volunteer. The heartbeat-induced motion artifact is clearly visible; its amplitude is similar to that in the retina (see Fig. 3A). (**C**) Typical measurement of the axial shift of the retina of 1 volunteer while the subject is lying down. Head movements are minimized and the heart rate is not visible.

In Figure 5, the frequency components in the OCT shift signal are plotted versus the heart rate (the frequency component caused by breathing is not shown in Fig. 5). It is clear that all frequency components of 27 measurements are either the fundamental frequency or higher order harmonic frequencies of the heartbeat. The number of detected higher order harmonics decreases with increasing order, because they were either too weak or the noise was too high. Note that for a very spiky periodic axial motion in time, such as for the measured axial motion of the retina, the frequency spectrum consists of a large number of harmonics. The result of the frequency analysis is in agreement with this sharply peaked axial motion artifact. We conclude that the axial motions in OCT imaging of the retina are caused by the heartbeat.

Axial motion artifacts during OCT measurements are often regarded as eye movements caused by microsaccades or unstable fixation.[23] We investigated the effect of lateral eye motions by rotating the eye several times from left to right over 8° during continuous OCT acquisition. No effect on the axial motion was observed, which is in agreement with gaze stability measurement reported in a previous study,[24] and it was also calculated[3] that the error of depth position for a rotation of approximately 1° for a healthy volunteer is smaller than 1.5 μm, which is lower than our resolution.

Figure 6A shows that the corneal surface moves in phase with the retinal surface, implying an entire head movement. However, the amplitude of the retinal movement is somewhat larger (especially at large movements). Note that for a whole head movement, the shifts of both the retina and the cornea should be similar as only the path length in air changes for both interfaces. However, the sensitivity measured on the retina is 22.1 dB lower with this configuration because of the use of the cylindrical lens in the sample arm (measured using a phantom eye model[20] with a mirror as retina). The observed difference between both amplitudes might therefore be related to the accuracy of the cross-correlation. The cross-correlation can be less accurate because the A-scan of the retina has multiple peaks with similar amplitude and lower signal-to-noise ratio. The A-scan of the cornea shows a strong single reflection at the air–cornea interface, and therefore its autocorrelation is more accurate.

Previous studies[25,26] showed that the axial length changes because of the heartbeat cycle. However, axial length changes during a heartbeat cycle that were measured with low coherence interferometry are in the order of 3.5 μm and are not in agreement with our results. Also, our axial resolution is limited by the optical bandwidth of the light source, and we are not able to measure axial length difference smaller than the coherence length. Heartbeat-related motions were furthermore confirmed in an animal study.[27] They showed that motions in the retina during OCT scanning can be caused by the heart rate. However, the measurements in this study were performed on rodents and the blood pressure was not synchronized with OCT scanning. Partially in agreement with our measurements, they found an identical movement of the cornea and retina both in phase but also in amplitude presumably caused by heartbeat, but the motions were not measured simultaneously. Also, they measure choroidal thickness changes during a heart beat cycle. This can be a very interesting topic for a successive study with a double reference arm OCT setup, because this can be an indicator for the progression of eye diseases that involve changes in perfusion of the retina. However, to do this we have to measure with larger wavelength for a larger penetration depth with OCT.

The effect of whole head movement was further investigated by OCT imaging on the teeth (Fig. 6B). The heartbeat-induced axial motion is clearly visible, and the amplitude is similar to what we measure on the retina.

Finally, we reduced the effect of the heart rate on head motions by performing OCT measurements on the retina when the subject was lying down. In this case, the head does not easily move toward the illuminating beam during the measurement, and heartbeat-induced motions of the head are therefore very much reduced during the measurement (Fig. 6C). This indicates that axial motions are mainly caused by movements of the head and probably not causing a compression of the eye. The measured amplitude of the retina or entire eye motion has a smaller amplitude than the amplitude of the whole head movement measured on the teeth. In our view, these small motions in Figure 6C, containing mainly 2.3 to 3.0 Hz motions, are unlikely to be caused by the heartbeat, and the motions are in disagreement with the amplitude and frequency of the shift in our earlier measurements (Fig. 6B). Our OCT setup provides the opportunity to investigate the origin of the remaining axial motions that are visible in Figure 6C (e.g., muscular contraction).

Based on our measurements, we conclude that the retinal axial motions are largely caused by an entire head movement that is caused by the heart rate. Axial motions are not movements of the whole eye within the eye socket, nor movements of the retina relative to the cornea (involving a compression/expansion of the eye). Although we measured different amplitudes between cornea and retina, we hypothesize that the heartbeat causes an arterial blood pressure pulse in the arteria carotis that induces a head movement that is translated to the eye and visible during OCT scanning of the retina. In summary, we have elucidated a major cause of imaging artifacts in OCT of the retina. Our results can help in a better quantification of (Doppler) OCT data and improve medical diagnosis with OCT.

References

1. Hedley M, Yan H. Motion artifact suppression: a review of post-processing techniques. *Magn Reson Imaging.* 1992;10:627–635.
2. Bellon EM, Haacke EM, Coleman PE, Sacco DC, Steiger DA, Gangarosa RE. MR artifacts: a review. *AJR Am J Roentgenol.* 1986;147:1271–1281.
3. Pircher M, Baumann B, Goetzinger E, Sattmann H, Hitzenberger CK. Simultaneous SLO/OCT imaging of the human retina with axial eye motion correction. *Opt Express.* 2007;15:16922–16932.
4. Zysk AM, Nguyen FT, Oldenburg AL, Marks DL, Boppart SA. Optical coherence tomography: a review of clinical development from bench to bedside. *J Biomed Opt.* 2007;12:051403.
5. Huang D, Swanson EA, Lin CP, et al. Optical coherence tomography. *Science.* 1991;254:1178–1181.
6. Jang IK, Bouma BE, Kang DH, et al. Visualization of coronary atherosclerotic plaques in patients using optical coherence tomography: comparison with intravascular ultrasound. *J Am Coll Cardiol.* 2002;39:604–609.
7. Mogensen M, Thrane L, Jørgensen TM, Andersen PE, Jemec GB. OCT imaging of skin cancer and other dermatological diseases. *J Biophotonics.* 2009;2:442–451.
8. Testoni PA, Mangiavillano B. Optical coherence tomography in detection of dysplasia and cancer of the gastrointestinal tract and bilio-pancreatic ductal system. *World J Gastroenterol.* 2008;14:6444–6452.
9. Cauberg ECC, de Bruin DM, Faber DJ, van Leeuwen TG, de la Rosette J, de Reijke TM. A new generation of optical diagnostics for bladder cancer: technology, diagnostic accuracy, and future applications. *Eur Urol.* 2009;56:287–296.
10. Mirza RG, Johnson MW, Jampol LM. Optical coherence tomography use in evaluation of the vitreoretinal interface: a review. *Surv Ophthalmol.* 2007;52:397–421.
11. van Velthoven MEJ, Faber DJ, Verbraak FD, van Leeuwen TG, de Smet MD. Recent developments in optical coherence tomography for imaging the retina. *Prog Retin Eye Res.* 2007;26:57–77.
12. Chen ZP, Milner TE, Srinivas S, et al. Noninvasive imaging of in vivo blood flow velocity using optical Doppler tomography. *Optics Letters.* 1997;22:1119–1121.

13. White BR, Pierce MC, Nassif N, et al. In vivo dynamic human retinal blood flow imaging using ultra-high-speed spectral domain optical Doppler tomography. *Opt Express.* 2003;11:3490–3497.
14. Potsaid B, Gorczynska I, Srinivasan VJ, et al. Ultrahigh speed Spectral/Fourier domain OCT ophthalmic imaging at 70,000 to 312,500 axial scans per second. *Opt Express.* 2008;16:15149–15169.
15. Choma MA, Sarunic MV, Yang CH, Izatt JA. Sensitivity advantage of swept source and Fourier domain optical coherence tomography. *Opt Express.* 2003;11:2183–2189.
16. de Boer JF, Cense B, Park BH, Pierce MC, Tearney GJ, Bouma BE. Improved signal-to-noise ratio in spectral-domain compared with time-domain optical coherence tomography. *Opt Letters.* 2003;28:2067–2069.
17. Leitgeb R, Hitzenberger CK, Fercher AF. Performance of Fourier domain vs. time domain optical coherence tomography. *Opt Express.* 2003;11:889–894.
18. Yun SH, Tearney GJ, de Boer JF, Bouma BE. Motion artifacts in optical coherence tomography with frequency-domain ranging. *Opt Express.* 2004;12:2977–2998.
19. Schmoll T, Kolbitsch C, Leitgeb RA. Ultra-high-speed volumetric tomography of human retinal blood flow. *Opt Express.* 2009;17:4166–4176.
20. de Bruin DM, Bremmer RH, Kodach VM, et al. Optical phantoms of varying geometry based on thin building blocks with controlled optical properties. *J Biomed Opt.* 2010;15:025001.
21. Grajciar B, Pircher M, Hitzenberger CK, Findl O, Fercher AF. High sensitive measurement of the human axial eye length in vivo with Fourier domain low coherence interferometry. *Opt Express.* 2008;16:2405–2414.
22. Makita S, Hong Y, Yamanari M, Yatagai T, Yasuno Y. Optical coherence angiography. *Opt Express.* 2006;14:7821–7840.
23. Ferguson RD, Hammer DX, Paunescu LA, Beaton S, Schuman JS. Tracking optical coherence tomography. *Opt Letters.* 2004;29:2139–2141.
24. Ferman L, Collewijn H, Jansen TC, Van den berg AV. Human gaze stability in the horizontal vertical and torsional direction during voluntary head movements, evaluated with a three-dimensional scleral induction coil technique. *Vision Res.* 1987;27:811–828.
25. Dragostinoff N, Werkmeister RM, Groschl M, Schmetterer L. Depth-resolved measurement of ocular fundus pulsations by low-coherence tissue interferometry. *J Biomed Opt.* 2009;14:054047.
26. Berisha F, Findl O, Lasta M, Kiss B, Schmetterer L. A study comparing ocular pressure pulse and ocular fundus pulse in dependence of axial eye length and ocular volume. *Acta Ophthalmol.* 2010;88:766–772.
27. Singh K, Dion C, Costantino S, Wajszilber M, Lesk MR, Ozaki T. Development of a novel instrument to measure the pulsatile movement of ocular tissues. *Exp Eye Res.* 2010;91:63–68.